Effect of Aluminum Source on Hydrothermal Synthesis of High-Silica Mordenite in Fluoride Medium, and It's Thermal Stability

Baowang Lu,† Tomohiro Tsuda,† Hitoshi Sasaki,† Yasunori Oumi,† Keiji Itabashi,‡ Toshiharu Teranishi,† and Tsuneji Sano*,†

School of Materials Science, Japan Advanced Institute of Science and Technology, Tatsunokuchi, Ishikawa 923-1292, Japan, and Nanyo Research Lab, Tosoh Corporation, Shunan, Yamaguchi 746-8501, Japan

Received July 22, 2003. Revised Manuscript Received October 28, 2003

Effect of an aluminum source on the direct hydrothermal synthesis of high-silica mordenite-type zeolite in the presence of tetraethylammonium and fluoride ions was investigated. Highly crystalline MOR-type zeolites with a Si/Al ratio of approximately 30 were successfully prepared using $Al(NO_3)_3$ as an aluminum source. To clarify the role of fluoride ions, NaF as a fluoride source was added in the course of crystallization process. It was found that the crystallinity and the Si/Al ratio of MOR-type zeolite do not depend on the addition time of NaF. However, the content of fluorine in the as-synthesized zeolite decreased markedly when NaF was added in the course of crystallization process. The decrease in fluorine content improved considerably the thermal stability of the as-synthesized MOR-type zeolite.

Introduction

Mordenite (MOR) type zeolite, one of the high-silica zeolites, has outstanding properties of high thermal and acid stabilities, and is an industrially important zeolite used in adsorptive separation and catalysis such as isomerization, alkylation, and hydrocracking.[1−3] Therefore, there is still an incentive to develop an effective method for synthesis of high-silica MOR-type zeolite. High-silica MOR-type zeolite is usually prepared through removal of aluminum from the zeolite framework by treatment with steam and/or acid. However, the dealuminated MOR-type zeolite is known to be less thermally stable than the directly synthesized high-silica MOR-type zeolite.[4] It is recognized that various organic structure-directing agents such as benzyltrimethylammonium hydroxide, tetraethylammonium hydroxide, hexamethyleneimine, and benzene-1,2-diol are very effective for the direct hydrothermal synthesis of high-silica MOR-type zeolite.[5−10] To our knowledge, however, the maximum Si/Al ratio reported in the literature is only 17.5.[7]

It is also well-known that addition of fluoride into the starting synthesis gel favors crystallization of high-silica zeolites.[11−21] Although fluoride anions have been considered to act as a mineralizing agent and/or a structure-directing agent,[22−28] the locations of fluoride anions and their influence on zeolite properties are still not clear.

* To whom correspondence should be addressed. E-mail: t-sano@jaist.ac.jp.
† Japan Advanced Institute of Science and Technology.
‡ Tosoh Corporation.

(1) Bajpai, P. K. *Zeolites* **1986**, *6*, 2.
(2) Maxwell, I. E.; Stork, W. H. J. *Introduction to Zeolite Science and Practice*; von Bekkum, H., Flanigen, E. M., Jonsen, J. C., Eds.; Elsevier: Amsterdam, The Netherlands, 1991; p 71.
(3) Fernandes, L. D.; Monteiro, J. L. F.; Sousa-Aguiar, E. F.; Martinez, A.; Corma, A. *J. Catal.* **1998**, *177*, 363.
(4) Beyer, H. K.; Belenykaja, I. M.; Mishin, I. W.; Borbely, G. In *Structure and Reactivity of Modified Zeolites*; Jacobs, P. A., Jaeger, N. I., Jiru, P., Kazansky, V. B., Schulz-Ekloff, G., Eds.; Elsevier: Amsterdam, The Netherlands, 1984; p 133.
(5) Ueda, S.; Fukushima, T.; Koizumi, M. *J. Clay Sci. Jpn.* **1982**, *22*, 18.
(6) Covini, R.; Genoni, F.; Levanmao, R.; Moretti, E.; Pilati, O. U.S. Patent 4,366,132, 1982.
(7) Shaikh, A. A.; Joshi, P. N.; Jacob, N. E.; Shiralkar, V. P. *Zeolites* **1993**, *13*, 511.
(8) Jongkind, H.; Datema, K. P.; Nabuurs, S.; Seive, A.; Stork, W. H. J. *Microporous Mater.* **1997**, *10*, 149.
(9) Qian, B.; Guo, G.; Wang, X.; Zeng, Y.; Sun, Y.; Long, Y. *Phys. Chem. Chem. Phys.* **2001**, *3*, 4164.
(10) Shao, C.; Kim, H.-Y.; Li, X.; Park, S.-J.; Lee, D.-R. *Mater. Lett.* **2002**, *56*, 24.
(11) Flanigen, E. M.; Patton, R. L. U.S. Patent 4,073,865, 1978.
(12) Guth, J. L.; Kessler, H.; Wey, R. In *Proceedings of the 7th International Zeolite Conference*; Murakami, Y., Iijima, A., Ward, J. W., Eds.; Elsevier: Amsterdam, 1986; p 121.
(13) Guth, J. L.; Kessler, H.; Caullet, P.; Hazm, J.; Merrouche, A.; Patarin, J. In *Proceedings from the 9th International Zeolite Conference*; von Ballmoos, R., Higgins, J. B., Tracy, M. M. L., Eds.; Butterworth-Heinemann: Stoneham, MA, 1993; p 215.
(14) Mostowicz, R.; Testa, F.; Crea, F.; Aiello, R.; Fonseca, A.; Nagy, J. B. *Zeolites* **1997**, *18*, 308.
(15) Camblor, M. A.; Villaescusa, L. A.; Diaz-Cabanas, M. J. *Top. Catal.* **1999**, *9*, 59.
(16) Qi, X.; Liu, X.; Wang, Z. *Stud. Surf. Sci. Catal.* **2001**, *135*, 02P39.
(17) Fyfe, C. A.; Brouwer, D. H.; Lewis, A. R.; Villaescusa, L. A.; Morris, R. E. *J. Am. Chem. Soc.* **2002**, *124*, 7770.
(18) Serrano, D. P.; Van Grieken, R.; Sanchez, P.; Sanz, R.; Rodriguez, L. *Microporous Mesoporous Mater.* **2001**, *46*, 35.
(19) Kato, M.; Itabashi, K.; Matsumoto, A.; Tsutsumi, K. *J. Phys. Chem. B* **2003**, *107*, 1788.
(20) Blasco, T.; Camblor, M. A.; Corma, A.; Esteve, P.; Guil, J. M.; Martinez, A.; Perdigon-Melon, J. A.; Valencia, S. *J. Phys. Chem. B* **1998**, *102*, 75.
(21) Camblor, M. A.; Corma, A.; Valencia, S. *J. Mater. Chem.* **1998**, *9*, 2137.
(22) Koller, H.; Wolker, A.; Eckert, H.; Panz, C.; Behrens, P. *Angew. Chem., Int. Ed. Engl.* **1997**, *36*, 2823.
(23) Koller, H.; Wolker, A.; Villaescusa, L. A.; Diaz-Cabanas, M. J.; Valencia, S.; Camblor, M. A. *J. Am. Chem. Soc.* **1999**, *121*, 3368.
(24) Bull, I.; Villaescusa, L. A.; Teat, S. J.; Camblor, M. A.; Wright, P. A.; Lightfoot, P.; Morris, R. E. *J. Am. Chem. Soc.* **2000**, *122*, 7128.

10.1021/cm030576y CCC: $27.50
Published on Web 12/25/2003

Table 1. Effect of Al Source on Direct Synthesis of MOR-Type Zeolite[a]

		chemical composition of starting gel				product (byproduct)					
					crystallization		bulk Si/Al ratio		BET surface area	pore volume	F content
sample	Al source	Si/Al	NaOH/Al	NaF/SiO_2	time (d)	phase	XRF	ICP	(m^2/g)	(cm^3/g)	(ppm)
1	$AlCl_3$	15	3	0	3	MOR	15.3	14.6	419	0.18	
2	$AlCl_3$	15	3	0.8	3	MOR	15.5	14.5	292	0.14	4,800
3	$AlCl_3$	20	3	0.8	3	MOR	17.8	17.2			
4	$AlCl_3$	20	4	0.8	3	MOR	17.9				
5	$AlCl_3$	25	5	0.8	3	MOR	21.0		356	0.18	3,100
6	$AlCl_3$	30	5	0.8	3	MOR	26.5	23.1	358	0.15	2,600
7	$AlCl_3$	35	6	0.8	3	MOR	25.1	24.2			1,800
8	$AlCl_3$	40	7	0.8	3	BEA(MFI)					
9	$Al(NO_3)_3$	15	3	0	3	MOR	16.2		420	0.20	
10	$Al(NO_3)_3$	15	3	0.8	3	MOR	15.6		283	0.17	4,500
11	$Al(NO_3)_3$	20	4	0.8	3	MOR	19.1				
12	$Al(NO_3)_3$	25	5	0.8	3	MOR	20.1				6,000
13	$Al(NO_3)_3$	30	6	0.8	3	MOR	26.1				
14	$Al(NO_3)_3$	35	5	0.8	5	MOR	31.0	28.8	298	0.13	2,700
15	$Al(NO_3)_3$	40	7	0.8	3	MOR(BEA)					
16	$Al(NO_3)_3$	40	9	0.8	3	MOR	30.1	28.3	302	0.14	2,000
17	$Al(NO_3)_3$	45	9	0.8	3	BEA(MFI)					
18	$Al_2(SO_4)_3$	15	3	0.8	3	BEA(MOR)					
19	$Al_2(SO_4)_3$	20	4	0.8	3	MOR(BEA)					
20	$Al_2(SO_4)_3$	25	5	0.8	3	MOR(BEA)					

[a] Synthesis conditions: $TEAOH/SiO_2 = 0.23$; $H_2O/SiO_2 = 7.4$; Crystallization temp. = 170 °C.

From such a viewpoint, we have now studied the direct hydrothermal synthesis of high-silica MOR-type zeolite in the fluoride medium. Very recently, highly crystalline MOR-type zeolites with a bulk Si/Al ratio of approximately 25 were successfully prepared using both tetraethylammonium hydroxide and NaF.[29] To get further information concerning our method of direct synthesis of high-silica MOR-type zeolite, we investigated effects of the aluminum source and the addition time of NaF, and report the results in this paper.

Experimental Section

Synthesis of High-Silica MOR-Type Zeolite using Different Aluminum Sources. The hydrothermal synthesis of MOR-type zeolite was carried out in the presence of fluoride using different aluminum sources, such as $AlCl_3 \cdot 6H_2O$ (Wako Pure Chemical, Japan, 98.0%), $Al(NO_3)_3 \cdot 9H_2O$ (Wako, 98.0%), and $Al_2(SO_4)_3 \cdot 16-18H_2O$ (Wako, 99.5%). The starting mixtures were prepared as follows. The aluminum source was mixed with an aqueous solution containing NaOH (Merck-Schuchardt, Germany, 99%) and tetraethylammonium hydroxide (TEAOH, Aldrich, Milwaukee, WI, 35 wt %). Then the precipitated hydrated silica (Nipsil, Nippon Silica Ind., Japan, SiO_2 = 88 wt %, H_2O = 12 wt %) was added to the mixture and was homogenized in a mortar. Finally, NaF (Wako, 99.0%) was added as a fluoride source, and homogenization was continued until a uniform gel was obtained. The chemical composition of the starting synthesis gel prepared was as follows: Si/Al = 15−45, $H_2O/SiO_2 = 7.4$, NaOH/Al = 3−9, $NaF/SiO_2 = 0.8$, $TEAOH/SiO_2 = 0.23$. The gel thus obtained was charged into a 30-cm^3 stainless steel autoclave equipped with a Teflon liner and kept at 170 °C for 3−5 days under static conditions. The solid product was filtered, washed thoroughly with 1000 cm^3 of deionized hot water (60 °C), dried overnight in an oven at 120 °C, and calcined at 500 °C for 10 h.

Synthesis of High-Silica MOR-Type Zeolite by NaF Addition in the Course of Crystallization Process. To reveal the role of fluoride ions on the hydrothermal synthesis of high-silica MOR-type zeolite, NaF as a fluoride source was added in the course of crystallization process. Namely, the NaF-free starting gel was hydrothermally treated at 170 °C for a certain period, and NaF was added into the gel after cooling. Then the autoclave containing the gel was quickly heated up to 170 °C again and the hydrothermal synthesis was continued until the total crystallization time reached 72 h.

Characterization. The solid products obtained were identified by X-ray diffraction (XRD, Rigaku RINT 2000). The bulk chemical compositions were measured by X-ray fluorescence (XRF, Philips spectrometer PW 2400) and inductively coupled plasma optical emission spectroscopy (ICP−OES, Seiko, SPS 7700). Fluorine content was determined by an ion-selective electrode after dissolution of the samples. The crystal morphology and the surface Si/Al ratio were measured by scanning electron microscopy (SEM, Hitachi S-4000) and energy-dispersive X-ray analysis (EDX) on a Horiba EMAX system attached to the microscope. ^{27}Al MAS NMR spectra of MOR-type zeolites calcined at 500 °C were recorded using a zirconia rotor of 7-mm diameter on a Varian VXP-400 at 104.2 MHz and ^{19}F MAS NMR spectra at 376.7 MHz. Nitrogen adsorption isotherms at −196 °C were measured using a conventional volumetric apparatus (Bel Japan BELSORP 28SA). Prior to adsorption measurements, the powder zeolites (ca. 0.1 g) were evacuated at 400 °C for 6 h.

Evaluation of Thermal Stability of High-Silica MOR-Type Zeolite. The thermal stabilities of the high-silica MOR-type zeolites obtained were evaluated by comparing the structural differences of samples before and after calcination at 900 °C for 1 h by XRD and ^{27}Al MAS NMR analyses. Prior to calcination, the sample was moisture-equilibrated over a saturated solution of NH_4Cl.

Results and Discussion

Effect of Aluminum Source. The direct synthesis of high-silica MOR-type zeolite was carried out by using various aluminum sources in the presence of NaF as a fluoride source. The results obtained with starting synthesis gels with various chemical compositions are summarized in Table 1. The pure MOR-type zeolite phase could be obtained when $AlCl_3$ and $Al(NO_3)_3$ were employed as an aluminum source, whereas beta (BEA)

(25) Attfield, M. A.; Weigel, S. J.; Taulelle, F.; Cheetham, A. K. *J. Mater. Chem.* **2000**, *10*, 2109.
(26) Fyfe, C. A.; Brouwer, D. H.; Lewis, A. R.; Chezeau, J. M. *J. Am. Chem. Soc.* **2001**, *123*, 6882.
(27) Corma, A.; Diaz-Cabanas, M. J.; Martinez-Triguero, J.; Rey, F.; Rius, J. *Nature* **2002**, *418*, 514.
(28) Sastre, G.; Vidal-Moya, J. A.; Blasco, T.; Rius, J.; Jorda, J. L.; Navarro, M. T.; Rey, F.; Corma, A. *Angew. Chem., Int. Ed.* **2002**, *41*, 4722.
(29) Sasaki, H.; Oumi, Y.; Itabashi, K.; Teranishi, T.; Lu, B.-W.; Sano, T. *J. Mater. Chem.* **2003**, *13*, 1173.

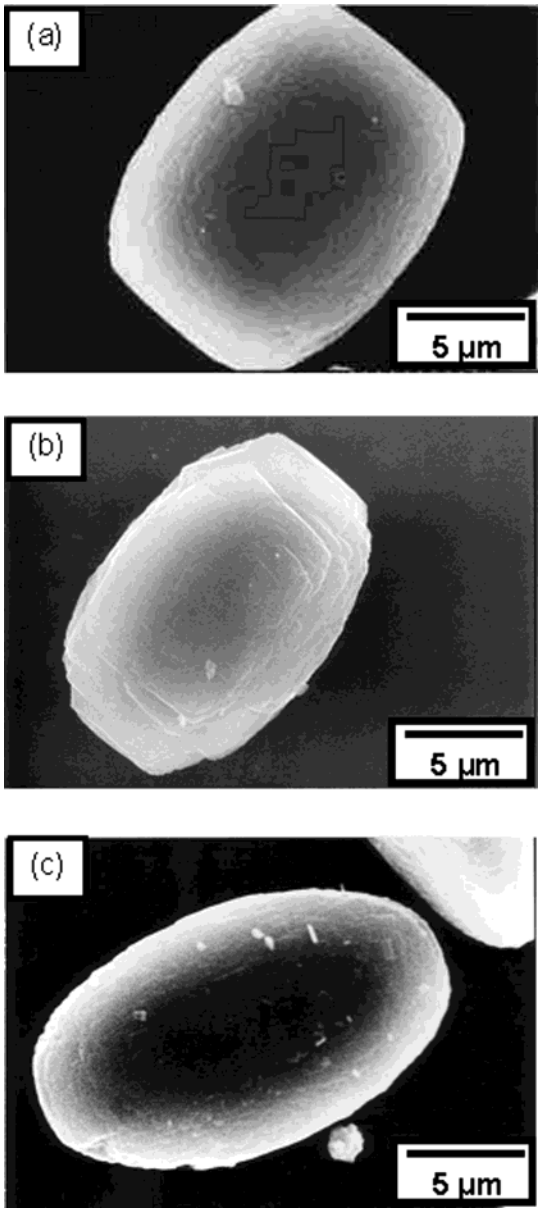

Figure 1. SEM images of MOR-type zeolites prepared using $AlCl_3$ and $Al(NO_3)_3$: (a) sample 2, (b) sample 10, and (c) sample 14.

type zeolite was prepared as a main product or a byproduct with $Al_2(SO_4)_3$. When the Si/Al ratio in the starting gel was increased, the pure MOR-type zeolite could be prepared with increasing the NaOH/Al ratio. For gels with a Si/Al ratio of more than 40 prepared using $AlCl_3$, MOR-type zeolite could not be synthesized even at the high NaOH/Al ratio, and BEA- and MFI-type zeolites were obtained. On the other hand, in the case of gels prepared using $Al(NO_3)_3$, highly crystalline MOR-type zeolites with a bulk Si/Al ratio of approximately 30 were successfully prepared (samples 14 and 16). The Si/Al ratios were confirmed again by the wet chemical analysis (ICP−OES). From our knowledge of direct synthesis of MOR-type zeolites, the Si/Al ratio of 30 is the highest value among those described in the literature. At the present time we could not explain the difference in the effect of aluminum source on the crystallization behavior because of limited data. The contents of fluorine in the as-synthesized zeolites measured by the ion-selective electrode are also listed in

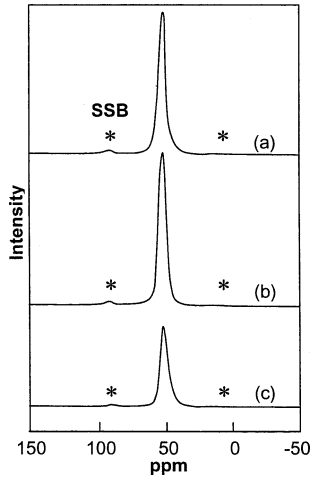

Figure 2. ^{27}Al MAS NMR spectra of MOR-type zeolites prepared using $AlCl_3$ and $Al(NO_3)_3$: (a) sample 2, (b) sample 10, and (c) sample 14.

Table 1. The fluorine content tends to decrease with an increase in the Si/Al ratio of the starting synthesis gel.

To obtain a qualitative assessment of microporosity of the obtained MOR-type zeolites, nitrogen adsorption isotherms were measured. As listed in Table 1, the BET surface area and the micropore volume determined by the Dubinin−Radushkevich equation of the MOR-type zeolite synthesized with NaF were slightly smaller than that of samples without NaF. As already reported in the previous paper, the smaller values are attributable to NaF present in the zeolite crystals.[29]

The typical SEM images of the high-silica MOR-type zeolites prepared are shown in Figure 1. Rectangular parallelepiped and rice-grain-like crystals were observed. ^{27}Al MAS NMR spectra of various zeolites calcined at 500 °C for 10 h are shown in Figure 2. The peak intensity was normalized based on 1 g of zeolite. Only a sharp signal at ca. 54 ppm was observed in the ^{27}Al MAS NMR spectra, which is a characteristic resonance of tetrahedrally coordinated framework aluminum species. No signal assigned to nonframework aluminum species (extraframework aluminum species) was observed around 0 ppm. Therefore, it was clearly revealed that all aluminums present in the high-silica MOR-type zeolites synthesized with NaF are present in the zeolite framework.

Effect of NaF Addition in the Course of Crystallization Process. To get a better understanding of the role of NaF, the high-silica MOR-type zeolite was synthesized by adding NaF to the synthesis gel in the course of crystallization process. The total crystallization time was fixed at 72 h. The results obtained are summarized in Table 2. In the case of the starting gels prepared with $AlCl_3$, the highly crystalline MOR-type zeolite was prepared even when NaF was added to the gel at 36 h of the crystallization time (sample 22). When the addition time of NaF was over 48 h, however, the synthesis gel was not crystallized completely. On the other hand, in the case of the starting gels prepared with $Al(NO_3)_3$, the synthesis gel was crystallized completely and the pure MOR-type zeolite was obtained even at 48 h of the NaF addition time (sample 27). Taking into account the fact that the synthesis gel without NaF was not crystallized completely at 72 h of

Table 2. Influence of NaF Addition in the Course of Crystallization Process of MOR-Type Zeolite[a]

	chemical composition of starting gel			product (byproduct)				
sample	Al source	NaF/SiO_2	addition time of NaF (h)	phase	bulk Si/Al ratio (XRF)	BET surface area (m^2/g)	pore volume (cm^3/g)	F content (ppm)
21	$AlCl_3$	0.8	18	MOR	22.8	379	0.19	800
22	$AlCl_3$	0.8	36	MOR	22.9	445	0.21	540
23	$AlCl_3$	0.8	48	MOR(am)				
24	$AlCl_3$	0		MOR(am)				
25	$Al(NO_3)_3$	0.8	18	MOR	20.8	361	0.18	1,400
26	$Al(NO_3)_3$	0.8	36	MOR	21.7	403	0.19	320
27	$Al(NO_3)_3$	0.8	48	MOR	21.1	420	0.21	260
28	$Al(NO_3)_3$	0		MOR(am)				

[a] Synthesis conditions: Si/Al = 25; NaOH/Al = 5; H_2O/SiO_2 = 7.4; TEAOH/SiO_2 = 0.23; crystallization temp. = 170 °C; crystallization time = 72 h.

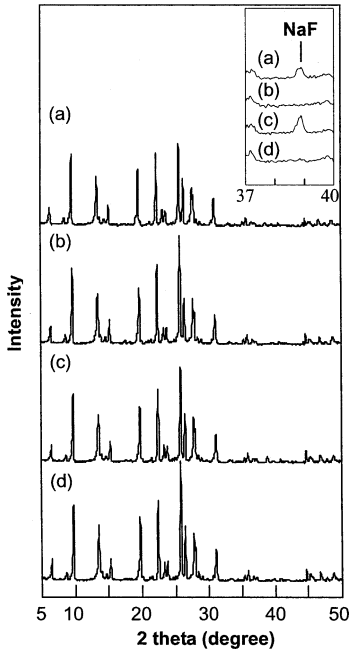

Figure 3. XRD patterns of MOR-type zeolites obtained by changing NaF addition time: (a) sample 5, (b) sample 22, (c) sample 12, and (d) sample 27.

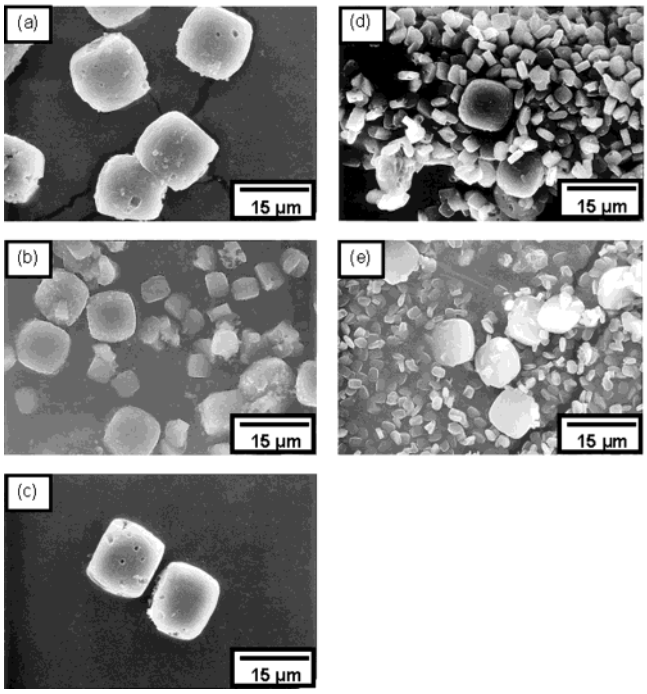

Figure 4. SEM images of MOR-type zeolites obtained by changing NaF addition time: (a) sample 5, (b) sample 22, (c) sample 12, (d) sample 26, and (e) MOR obtained at the crystallization condition of sample 26 without addition of NaF.

the crystallization time (samples 24 and 28), the addition of NaF into the synthesis gel was found to enhance the crystallization rate.

Figure 3 shows the typical XRD patterns of the as-synthesized MOR-type zeolites obtained at different addition times of NaF in the range 0−48 h. All samples gave no peaks other than those corresponding to a MOR-type zeolite. The very weak diffraction peak at 2θ ca. 38.9° assigned to NaF, as well as those from MOR-type zeolite, could be observed in the XRD patterns of the zeolites synthesized from the starting gels with NaF (samples 5 and 12). However, the diffraction peak of NaF was hardly observed in the XRD patterns of the zeolites obtained by adding NaF in the course of crystallization process (samples 22 and 27). The contents of fluorine in the as-synthesized zeolites measured by the ion-selective electrode are listed in Table 2. As expected, the fluorine content in the MOR-type zeolite obtained by adding NaF during crystallization was considerably smaller than that from the starting gel with NaF (Tables 1 and 2) and tended to decrease with the NaF addition time. This indicates that the content of the fluorine in the as-synthesized MOR-type zeolite is strongly dependent on the addition time of fluoride.

Figure 4 shows the SEM images of various MOR-type zeolites obtained at different addition times of NaF. The MOR-type zeolites synthesized from the starting gel with NaF had rectangular parallelepiped crystals and their crystals are ca. 15 μm long. On the other hand, in the SEM images of the MOR-type zeolites obtained by adding NaF in the course of crystallization process (Figure 4(b) and (d)), many small crystals other than a few large crystals were observed (samples 22 and 26). As we could not see any amorphous phase in the SEM images, this seems to suggest an enhancement of nucleation relative to small MOR-type zeolite crystals by NaF addition. However, there is another possibility that the new nucleation comes rather from the procedure of NaF addition. The temperature decrease, which is necessary to allow the introduction of NaF, favors the supersaturation of the MOR-type zeolite crystallization system. To clarify this, therefore, an influence of the temperature decrease was studied by using the synthesis 26 without addition of NaF. As shown in Figure 4(e), both small and large zeolite crystals were observed and the crystal sizes were smaller than those of the crystals obtained by addition of NaF. It was found that the new

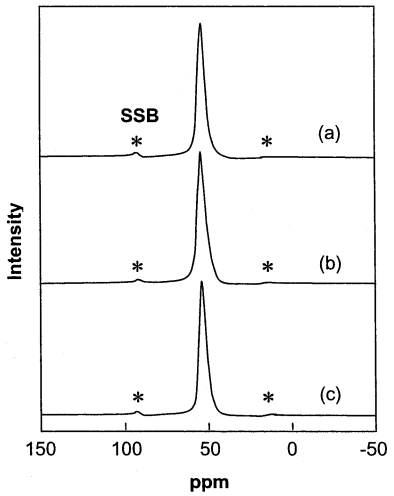

Figure 5. ^{27}Al MAS NMR spectra of MOR-type zeolites obtained by changing NaF addition time: (a) sample 5, (b) sample 21, and (c) sample 22.

nucleation is caused by the temperature decrease. The large crystals are probably due to the MOR-type zeolite crystals, which already existed in the gel before NaF addition. The surface Si/Al ratios measured by EDX were roughly 11−15, indicating an enrichment of Al on the crystal surface. However, there was no difference in the surface Si/Al ratio between large and small crystals.

Figure 5 shows the ^{27}Al MAS NMR spectra of various MOR-type zeolites obtained at different addition times of NaF. For all samples, only the peak of ca. 54 ppm assigned to tetrahedrally coordinated framework aluminums was observed, indicating that all aluminums in the as-synthesized MOR-type zeolites exist within the zeolite framework.

Recently, several research groups, using solid-state NMR and X-ray diffraction, have found a pentacoordinated silicon unit ($SiO_4/_2F^-$) in various as-synthesized zeolites such as MFI- and MTW-type zeolites.[22,23] In addition, it has also been found that fluoride anions are occluded in a double four-membered ring of as-synthesized zeolites such as AST, ISV, ITH, and ITW.[30−33] To get information concerning the chemical state of fluoride in the MOR-type zeolites obtained at different addition times of NaF, therefore, the ^{19}F MAS NMR spectra of the as-synthesized zeolites were measured. As shown in Figure 6 (a), only one peak was observed at ca. −72 ppm in the spectrum of MOR-type zeolite synthesized from the starting gel with NaF. This peak could be assigned to NaF (Figure 6(d)). In the ^{19}F MAS NMR spectra of the MOR-type zeolites synthesized by adding NaF in the course of crystallization process, no peak assigned to NaF was observed due to the low content of NaF (Figure 6(b) and (c)). Therefore, it became clear that the chemical state of fluoride ions in the high-silica MOR-type zeolites obtained is different from that in various zeolites synthesized in fluoride medium so far.

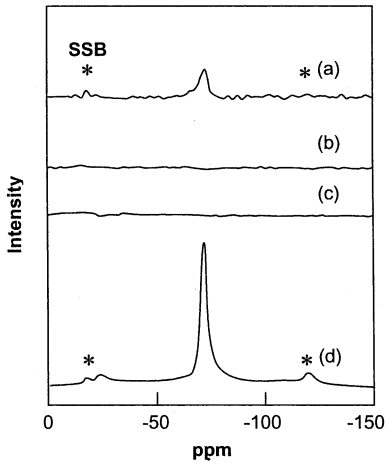

Figure 6. ^{19}F MAS NMR spectra of MOR-type zeolites and NaF: (a) sample 5, (b) sample 21, (c) sample 22, and (d) NaF.

Namely, the fluoride present in the as-synthesized MOR-type zeolites exists as NaF, and the amount of NaF is strongly affected by the addition time of NaF. As the pore size of mordenite is too small for the formation of crystalline NaF, the crystalline NaF is probably present as inclusions between the domains, which form big mordenite crystals and where its extraction is difficult by a simple washing. This is not the case for mordenite crystals obtained by NaF addition in the course of crystallization process. Due to very small size, there are less inclusions and they are more easily extracted by washing.

Thermal Stability. The XRD and ^{27}Al MAS NMR analyses were used to study the thermal stability of the MOR-type zeolites synthesized by adding NaF in the course of crystallization process. The XRD spectra of the MOR-type zeolites before and after calcination at 900 °C are shown in Figure 7. In the case of the MOR-type zeolite synthesized from the starting gel with NaF, the XRD peak intensities corresponding to MOR-type zeolite decreased dramatically after calcination, and only diffraction peaks from cristobalite were observed. On the other hand, in the case of MOR-type zeolite obtained at 36 h of the NaF addition time, the XRD peak intensities after calcination are almost the same as those before calcination. Figure 8 shows the ^{27}Al MAS NMR spectra of the MOR-type zeolites before and after calcination. The marked decrease in the peak intensity at ca. 54 ppm was observed for the zeolite prepared from the starting gel with NaF, whereas no decrease occurred in the peak intensity for the zeolite prepared by adding NaF during crystallization. These results suggest that the thermal stability of the as-synthesized high-silica MOR-type zeolite is strongly dependent on the addition time of NaF. In our previous paper, the low thermal stability of MOR-type zeolite prepared in the presence of NaF was found to be attributable to NaOH (or Na_2O) formed by the reaction between NaF and silanol groups in the zeolite during calcination at 900 °C, which led to the structural degradation of MOR-type zeolite by alkali fusion.[29] Therefore, it may be concluded that the higher thermal stability of MOR-type zeolites obtained by adding NaF in the course of crystallization process is due to the lower content of NaF in their crystals.

Next, to evaluate the thermal stability of the high-silica MOR-type zeolite accurately, the as-synthesized

(30) Caullet, P.; Guth, J. L.; Hazm, J.; Lamblin, J. M.; Gies, H. *Eur. J. Solid State Inorg. Chem.* **1991**, *28*, 345.
(31) Villaescusa, L. A.; Barrett, P. A.; Camblor, M. A. *Angew. Chem., Int. Ed.* **1999**, *38*, 1997.
(32) Corma, A.; Puche, M.; Rey, F.; Sankar, G.; Teat, S. J. *Angew. Chem., Int. Ed.* **2003**, *42*, 1156.
(33) Barrett, P. A.; Boix, T.; Puche, M.; Olson, D. H.; Jordan, E.; Koller, H.; Camblor, M. A. *Chem. Commun.* **2003**, 2114.

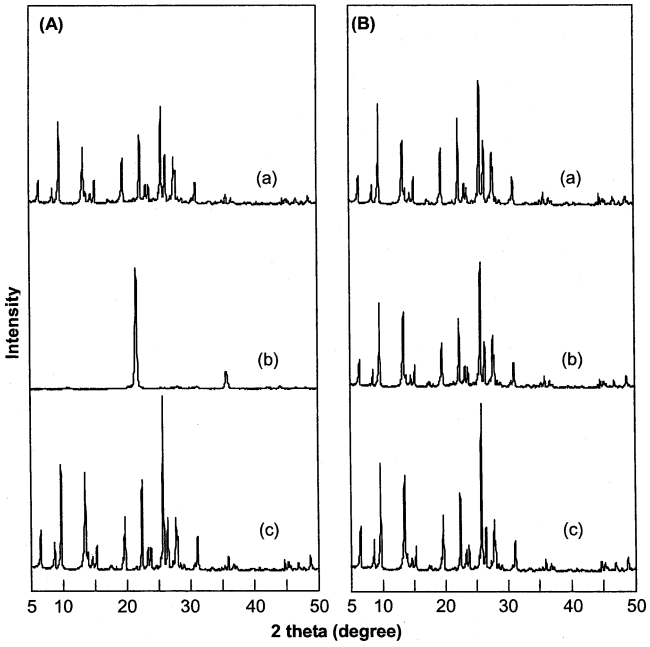

Figure 7. XRD patterns of various MOR-type zeolites: (A) sample 5 and (B) sample 22. (a) MOR calcined at 500 °C for 10 h. (b) Sample (a) was calcined at 900 °C for 1 h. (c) As-synthesized MOR was treated hydrothermally at 170 °C for 2 days (3×), calcined at 500 °C for 10 h, and then calcined at 900 °C for 1 h.

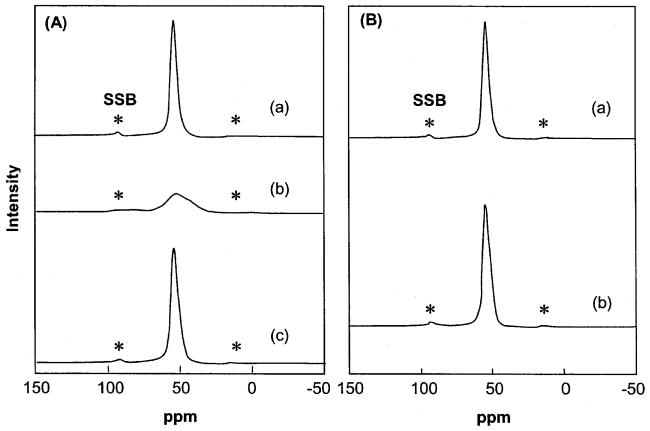

Figure 8. ^{27}Al MAS NMR spectra of various MOR-type zeolites: (A) sample 5, and (B) sample 22. (a) MOR calcined at 500 °C for 10 h. (b) Sample (a) was calcined at 900 °C for 1 h. (c) As-synthesized MOR was treated hydrothermally at 170 °C for 2 days (3×), calcined at 500 °C for 10 h, and then calcined at 900 °C for 1 h.

zeolite was hydrothermally treated at 170 °C for 2 days to remove NaF. This procedure was repeated 3× until the peak corresponding to NaF at 2θ ca. 38.9° was not observed in the XRD pattern. The fluorine contents in the MOR-type zeolite after the hydrothermal treatment were below 100 ppm. As shown in Figures 7(c) and 8(c), the thermal stability was dramatically improved by the hydrothermal treatment. Figure 9 illustrates the relationship between the bulk Si/Al ratio and the relative crystallinity for various MOR-type zeolites after calcination at 900 °C for 1 h. The relative crystallinity was defined as follows.

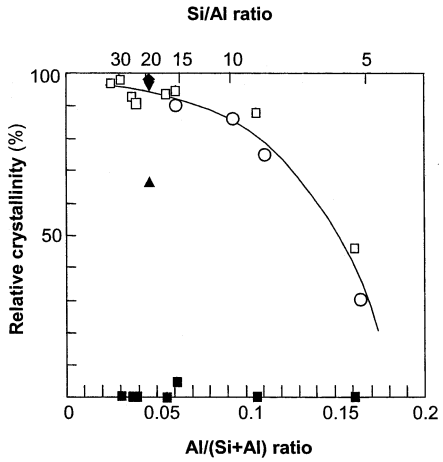

Figure 9. Relationship between bulk Si/Al ratio and relative crystallinity of MOR-type zeolite after calcination at 900 °C for 1 h. (■) MOR synthesized from starting gel with NaF; (□) MOR after hydrothermal treatment at 170 °C; (○) MOR synthesized without NaF; (▲) MOR synthesized at 18 h of NaF addition time (sample 21); (▼) MOR synthesized at 36 h of NaF addition time (sample 22); and (◆) MOR synthesized at 48 h of NaF addition time (sample 27).

Relative crystallinity (%) =
(Sum of area under the peaks between 2 theta = 5 − 40 after calcination at 900 °C for 1 h)/
(Sum of area under the peaks between 2 theta = 5 − 40 after calcination at 500 °C for 10 h) × 100

In the case of the MOR-type zeolite synthesized without NaF, a good relationship was observed between the bulk Si/Al ratio and the relative crystallinity. Namely, the thermal stability of the MOR-type zeolite was increased with an increase in bulk Si/Al ratio. On the other hand, the thermal stability of MOR-type zeolites synthesized in the presence of NaF depended strongly on the addition time of NaF. The data for the hydrothermally treated MOR-type zeolite were fitted to a common curve of those without NaF, indicating a marked enhancement in thermal stability.

Conclusions

Under well-optimized conditions, highly crystalline MOR-type zeolites with a Si/Al ratio of approximately 30 were successfully prepared when $Al(NO_3)_3$ was employed as an aluminum source. The Si/Al ratio was the highest value among MOR-type zeolites reported so far. It was also found that the addition of NaF to the synthesis gel in the course of crystallization process enhances the growth rate of MOR-type zeolite and that the fluoride ions are present in the as-synthesized MOR-type zeolite as NaF. The amount of NaF remaining in the MOR-type zeolites decreased with the NaF addition time, resulting in the enhancement of their thermal stability.

CM030576Y